

Online Limited Memory Neural-Linear Bandits with Likelihood Matching

Ofir Nabati¹ Tom Zahavy¹ Shie Mannor¹

Abstract

We study neural-linear bandits for solving problems where *both* exploration and representation learning play an important role. Neural-linear bandits leverage the representation power of Deep Neural Networks (DNNs) and combine it with efficient exploration mechanisms designed for linear contextual bandits on top of the last hidden layer. A recent analysis of DNNs in the “infinite-width” regime suggests that when these models are trained with gradient descent the optimal solution is close to the initialization point and the DNN can be viewed as a kernel machine. As a result, it is possible to exploit linear exploration algorithms on top of a DNN via the kernel construction. The problem is that in practice the kernel changes during the learning process and the agent’s performance degrades. This can be resolved by recomputing new uncertainty estimations with stored data. Nevertheless, when the buffer’s size is limited, a phenomenon called catastrophic forgetting emerges. Instead, we propose a likelihood matching algorithm that is resilient to catastrophic forgetting and is completely online. We perform simulations on a variety of datasets and observe that our algorithm achieves comparable performance to the unlimited memory approach while exhibits resilience to catastrophic forgetting.

1. Introduction

Deep neural networks (DNNs) can learn complex representations of data and have dramatically improved the state-of-the-art in speech recognition, visual object recognition, object detection, and many other domains such as drug discovery and genomics (LeCun et al., 2015; Goodfellow et al., 2016). Using DNNs for function approximation in reinforcement learning (RL) enables the agent to generalize

across states without domain-specific knowledge and learn rich domain representations from raw, high-dimensional inputs (Mnih et al., 2015; Silver et al., 2016). Nevertheless, the question of how to perform efficient exploration during the representation learning phase is still an open problem. The ϵ -greedy policy (Langford & Zhang, 2008) is simple to implement and widely used in practice (Mnih et al., 2015). However, it is statistically suboptimal. Optimism in the Face of Uncertainty (OFU) uses confidence sets to balance exploitation and exploration (Abbasi-Yadkori et al., 2011; Auer, 2002) while Thompson Sampling (TS) does so by choosing optimal action with respect to a sampled belief of the model. (Thompson, 1933; Agrawal & Goyal, 2013). For DNNs, such confidence sets may not be accurate enough to allow efficient exploration. For example, using dropout as a posterior approximation for exploration does not concentrate on observed data (Osband et al., 2018) and was shown empirically to be insufficient (Riquelme et al., 2018). Alternatively, pseudo-counts, a generalization of the number of visits, were used as an exploration bonus (Bellemare et al., 2016; Pathak et al., 2017). Inspired by tabular RL, these ideas ignore the uncertainty in the value function approximation in each context. As a result, they may lead to inefficient confidence sets (Osband et al., 2018).

Linear models, on the other hand, are considered more stable and provide accurate uncertainty estimates but require substantial feature engineering to achieve good results. Additionally, they are known to work in practice only with “medium-sized” inputs (with around 1,000 features) due to numerical issues. A natural attempt at getting the best of both worlds is to learn a linear exploration policy on top of the last hidden layer of a DNN, which we term the **neural-linear** approach. In RL, this approach was shown to refine the performance of DQNs (Levine et al., 2017) and improve exploration when combined with TS (Aizzadenesheli et al., 2018) and OFU (O’Donoghue et al., 2018; Zahavy et al., 2018a). For contextual bandits, Riquelme et al. (2018) showed that neural-linear TS achieves superior performance on multiple datasets.

A practical challenge for neural-linear bandits is that the representation (the activations of the last hidden layer) change after every optimization step, while linear contextual bandits algorithms assume the features are stationary. A recent line of works (Zhou et al., 2020; Zhang et al., 2020; Xu et al.,

¹Department of Electrical-Engineering, Technion Institute of Technology, Israel. Correspondence to: Ofir Nabati <ofir-nabati@gmail.com>.

2020) analyze deep contextual bandits in the infinite width regime, in which networks behave as a linear kernel method. This kernel is known as the Neural Tangent Kernel (NTK) (Jacot et al., 2018). Under the NTK assumption, the optimal solution (and its features) is guaranteed to be close to the initialization point, which implies that representation barely changes during training when neural bandits scheme is used. Under these assumptions, the authors of Zhou et al. (2020) showed that the regret of a neural bandit is not larger than $\tilde{O}(\sqrt{T})$ at round T with a high probability.

Riquelme et al. (2018), on the other hand, observed that with standard DNN architectures, there is a change at these features during training (representation drift), and a mechanism to adapt for that change is required. They tackled this problem by storing the entire dataset in a memory buffer and computing new features for all the data after each DNN learning phase. The authors also experimented with a bounded memory buffer but observed a significant decrease in performance due to **catastrophic forgetting** (Kirkpatrick et al., 2017), i.e., a loss of information from previous experience.

In this work, we propose a complementary approach that can be added on top of the previously mentioned algorithms to tackle the representation drift problem with small memory usage while being resilient to the catastrophic forgetting. The key to our approach is a novel method to compute priors whenever the DNN features change. Specifically, we adjust the moments of the reward estimation conditioned on new features to match the likelihood conditioned on old features. We achieve this by solving a semi-definite program (Vandenberghe & Boyd, 1996, SDP) to approximate the covariance and using the weights of the last layer as a prior to the mean. This way, we narrow the representation drift between network updates while using limited memory. While our approach can be used for OFU based algorithms, we focus on the TS approach. To make the algorithm more appealing for real-time usage, we implement it in an online manner, in which updates of the DNN weights and the priors are done simultaneously every step by using stochastic gradient descent (SGD) followed by projection of the priors. This obviates the need to process the whole memory buffer after each DNN learning phase and keeps our algorithm’s computational burden small.

We performed experiments on several real-world and simulated datasets, using Multi-Layered Perceptrons (MLPs). These experiments suggest that our prior approximation scheme improves performance significantly when memory is limited and shows an advantage over the NTK based algorithms. We demonstrate that our neural-linear bandit performs well in a sentiment analysis dataset where the input is high dimensional natural language, and we use a Convolution Neural Network (CNN). In this regime, it is

not feasible to use a linear method due to computational problems.

The proposed algorithm is the first neural-linear algorithm that is resilient to catastrophic forgetting due to limited memory to the best of our knowledge. In addition, unlike Riquelme et al. (2018), which uses multiple iterations per learning phase, our algorithm can be configured to work in an online manner, in which the DNN and statistics are efficiently updated each step.

2. Background

The stochastic, contextual (linear) multi-armed bandit problem. At every round $t = 1, 2, 3, \dots, T$, a contextual bandit algorithm observes a context $b(t)$ and chooses an arm $a(t) \in [1, \dots, N]$. The bandit can use the history H_{t-1} to make its decisions, where $H_{t-1} = \{b(\tau), a(\tau), r_{a(\tau)}(\tau), \tau = 1, \dots, t-1\}$, and $a(\tau)$ denotes the arm played at time τ . Most existing works typically make the following **realizability** assumption (Chu et al., 2011; Abbasi-Yadkori et al., 2011; Agrawal & Goyal, 2013).

Assumption 1. *The reward for arm i at time t is generated from an (unknown) distribution s.t. $\mathbb{E}[r_i(t)|b(t), H_{t-1}] = \mathbb{E}[r_i(t)|b(t)] = b(t)^\top \mu_i$, where $\{\mu_i \in \mathbb{R}^d\}_{i=1}^N$ are fixed but unknown.*

Let $a^*(t)$ denote the optimal arm at time t , i.e. $a^*(t) = \arg \max_i b(t)^\top \mu_i$, and let $\Delta_i(t)$ denote the difference between the mean rewards of the optimal arm and of arm i at time t , i.e., $\Delta_i(t) = b(t)^\top \mu_{a^*(t)} - b(t)^\top \mu_i$. The objective is to minimize the total regret $R(T) = \sum_{t=1}^T \Delta_{a(t)}$, where T is finite.

Algorithm 1 TS for linear contextual bandits

```

 $\forall i \in [1.., N]$ , set  $\Phi_i = I_d, \hat{\mu}_i = 0_d, \psi_i = 0_d$ 
for  $t = 1, 2, \dots$ , do
     $\forall i \in [1.., N]$ , sample  $\tilde{\mu}_i$  from  $N(\hat{\mu}_i, \nu^2 \Phi_i^{-1})$ 
    Play arm  $a(t) := \underset{i}{\operatorname{argmax}} b(t)^\top \tilde{\mu}_i$ 
    Observe reward  $r_t$ 
    Update:
         $\Phi_{a(t)} = \Phi_{a(t)} + b(t)b(t)^\top$ 
         $\psi_{a(t)} = \psi_{a(t)} + b(t)r_t, \hat{\mu}_{a(t)} = \Phi_{a(t)}^{-1} \psi_{a(t)}$ 
end for
    
```

TS for linear contextual bandits. Thompson sampling is an algorithm for online decision problems where actions are taken sequentially in a manner that must balance between exploiting what is known to maximize immediate performance and investing to accumulate new information that may improve future performance (Russo et al., 2018; Lattimore & Szepesvári, 2018). For linear contextual bandits, TS was introduced by Agrawal & Goyal (2013) and is

presented in Algorithm 1.

Suppose that the **likelihood** of reward $r_i(t)$, given context $b(t)$ and parameter μ_i , was given by the pdf of Gaussian distribution $Pr(r_i(t)|b(t), \mu_i) \sim \mathcal{N}(b(t)^\top \mu_i, \nu^2)$, and let $\Phi_i(t) = \Phi_i^0 + \sum_{\tau=1}^{t-1} b(\tau)b(\tau)^\top 1_{i=a(\tau)}$, $\hat{\mu}_i(t) = \Phi_i^{-1}(t) \sum_{\tau=1}^{t-1} b(\tau)r_{a(\tau)}(\tau) 1_{i=a(\tau)}$, where 1 is the indicator function and Φ_i^0 is the precision prior. Given a Gaussian **prior** for arm i at time t , $\mathcal{N}(\hat{\mu}_i(t), \nu^2 \Phi_i^{-1}(t))$, the **posterior** distribution at time $t+1$ is given by,

$$\begin{aligned} Pr(\tilde{\mu}_i|r_i(t), b(t)) &\propto Pr(r_i(t)|b(t), \tilde{\mu}_i)Pr(\tilde{\mu}_i) \\ &\propto \mathcal{N}(\hat{\mu}_i(t+1), \nu^2 \Phi_i^{-1}(t+1)). \end{aligned}$$

At each time step t , the algorithm generates samples $\{\tilde{\mu}_i(t)\}_{i=1}^N$ from the posterior distribution $\mathcal{N}(\hat{\mu}_i(t), \nu^2 \Phi_i^{-1}(t))$, plays the arm i that maximizes $b(t)^\top \tilde{\mu}_i(t)$ and updates the posterior. TS is guaranteed to have a total regret at time T that is not larger than $O(d^{3/2}\sqrt{T})$, which is within a factor of \sqrt{d} of the information-theoretic lower bound for this problem. It is also known to achieve excellent empirical results (Lattimore & Szepesvári, 2018). Although that TS often regarded as a Bayesian approach, the description of the algorithm and its analysis are prior-free, i.e., the regret bounds will hold irrespective of whether or not the actual reward distribution matches the Gaussian likelihood function used to derive this method (Agrawal & Goyal, 2013).

3. Our approach

Algorithm. Our algorithm is composed of four main components: **(1) Representation:** A DNN takes the raw context as an input and is trained to predict the reward of each arm; **(2) Exploration:** a mechanism that uses the last layer activations of the DNN as features and performs linear TS on top of them; **(3) Memory:** a buffer that stores previous experience; **(4) Likelihood matching:** a mechanism that uses the memory buffer and the DNN to account for changes in representation. Our full algorithm is presented in the Supplementary Material.

To derive our algorithm, we make a **soft realizability assumption**, which is a stronger assumption than Assumption 1. The difference is that we assume that **all** the representations produced by the DNN during training are **realizable** to some degree.

Assumption 2. For any representation ϕ that is produced by the DNN during training with loss 1, the reward for arm i at time t is generated from an (unknown) distribution s.t. $\mathbb{E}[r_i(t)|\phi(t), H_{t-1}] = \mathbb{E}[r_i(t)|\phi(t)]$ and $|\mathbb{E}[r_i(t)|\phi(t)] - \phi(t)^\top \mu_i| \leq \epsilon \quad \forall t$, where $\{\mu_i \in \mathbb{R}^d\}_{i=1}^N$ are fixed but unknown parameters and $\epsilon \geq 0$.

That is, for each representation, there exists a *different* linear

coefficients vector such that the expected reward is approximately linear in the features. While this assumption may be too strong to hold in practice, it allows us to derive our algorithm as a good approximation that performs exceptionally well on many problems. We now explain how each of these components works.

1. Representation. Our algorithm uses a DNN, denoted by f_ω , where ω represents the DNN's weights (for convenience, we omit the weight notation for the rest of the paper). The DNN takes the raw context $b(t) \in \mathbb{R}^d$ as its input. The network has N outputs that correspond to the estimation of the reward of each arm, given context $b(t) \in \mathbb{R}^d$, $f(b(t))_i$ denotes the estimation of the reward of the i -th arm.

Using a DNN to predict each arm's reward allows our algorithm to learn a nonlinear representation of the context. This representation is later used for exploration by performing linear TS on top of the last hidden layer activations. We denote the activations of the last hidden layer of f applied to this context as $\phi(t) = \text{LastLayerActivations}(f(b(t)))$, where $\phi(t) \in \mathbb{R}^g$. The context $b(t)$ represents raw measurements that can be high dimensional (e.g., image or text), where the size of $\phi(t)$ is a design parameter that we choose to be smaller ($g < d$). This makes contextual bandit algorithms practical for such datasets.

1.1 Training. Every iteration, we train f for P mini-batches. Training is performed by sampling experience tuples $\{b(\tau), a(\tau), r_{a(\tau)}(\tau)\}$ from the replay buffer E (details below) and minimizing the mean squared error (MSE),

$$\mathcal{L}_{NN}(\omega) = \|f_\omega(b(\tau))_{a(\tau)} - r_{a(\tau)}(\tau)\|_2^2, \quad (1)$$

where $r_{a(\tau)}$ is the reward that was received at time τ after playing arm $a(\tau)$ and observing context $b(\tau)$. Notice that only the output of arm $a(\tau)$ is differentiated, and that the DNN (including the last layer) is trained end-to-end to minimize Eq 1.

2. Exploration. Exploration is performed using the representation ϕ . Similar to the linear case, we assume that, given ϕ and μ , the likelihood of the reward is Gaussian. At each time step t , the agent observes a raw context $b(t)$ and uses the DNN f to produce a feature vector $\phi(t)$. The features $\phi(t)$ are used to perform linear TS, similar to Algorithm 1, but instead of using a Gaussian posterior, we use the Bayesian Linear Regression (BLR) formulation that was suggested in (Riquelme et al., 2018). Empirically, this update scheme was shown to converge to the true posterior and demonstrated excellent empirical performance (Riquelme et al., 2018).

In BLR, the noise parameter ν (Alg. 1) is replaced with a prior belief that is being updated over time. The **prior** for arm i at time t is given by $Pr(\tilde{\mu}_i, \tilde{\nu}_i^2) = Pr(\tilde{\nu}_i^2)Pr(\tilde{\mu}_i|\tilde{\nu}_i^2)$, where $Pr(\tilde{\nu}_i^2)$ is an inverse-gamma dis-

tribution $\text{Inv-Gamma}(a_i(t), b_i(t))$, and the conditional prior density $\Pr(\tilde{\mu}_i|\tilde{\nu}_i^2)$ is a normal distribution, $\Pr(\tilde{\mu}_i|\tilde{\nu}_i^2) \propto \mathcal{N}(\tilde{\mu}_i(t), \tilde{\nu}_i^2 \Phi_i(t)^{-1})$. Combining this prior with a Gaussian likelihood guarantees that the **posterior** distribution at time $\tau = t + 1$ is given in the same form (a conjugate prior), i.e., $\Pr(\tilde{\nu}_i) = \text{Inv-Gamma}(A_i(\tau), B_i(\tau))$ and $\Pr(\tilde{\mu}_i|\tilde{\nu}_i) = \mathcal{N}(\hat{\mu}_i(\tau), \tilde{\nu}_i^2 \Phi_i(\tau)^{-1})$.

In each step and for each arm $i \in 1..N$, we sample a noise parameter $\tilde{\nu}_i^2$ from $\Pr(\tilde{\nu}_i^2)$ and then sample a weight vector $\tilde{\mu}_i$ from the posterior $\mathcal{N}(\hat{\mu}_i, \tilde{\nu}_i^2(\Phi_i^0 + \Phi_i)^{-1})$. Once we sampled a weight vector for each arm, we choose to play arm $a(t) = \arg \max_i \phi(t)^T \tilde{\mu}_i$, and observe reward $r_{a(t)}(t)$. This is followed by a posterior update step:

$$\begin{aligned}\Phi_{a(t)} &= \Phi_{a(t)}^0 + \Phi_{a(t)} + \phi(t)\phi(t)^\top, \\ \psi_{a(t)} &= \psi_{a(t)} + \phi(t)r_{a(t)}, \\ \hat{\mu}_{a(t)} &= (\Phi_{a(t)})^{-1}(\Phi_{a(t)}^0 \mu_{a(t)}^0 + \psi_{a(t)}), \\ R_i^2(t) &= R_i^2(t-1) + r_i^2, \\ A_i(t) &= A_{a(t)}^0 + \frac{t}{2}, \\ B_i(t) &= B_{a(t)}^0 + \frac{1}{2}(R_i^2(t) + (\mu_{a(t)}^0)^\top \Phi_{a(t)}^0 \mu_{a(t)}^0 \\ &\quad - \hat{\mu}_{a(t)}(t)^\top \Phi_{a(t)}(t) \hat{\mu}_{a(t)}(t)).\end{aligned}$$

We note that the exploration mechanism only chooses actions; it **does not change** the DNN's weights.

3. Memory. After an action $a(t)$ is played at time t , we store the experience tuple $\{b(t), a(t), r_{a(t)}(t)\}$ in a finite memory buffer of size n that we denote by E . Once E is full, we remove tuples from E in a FIFO manner, i.e., we remove the first tuple in E with $a = a(t)$.

4. Likelihood matching. After each training phase, we evaluate the features of f on the replay buffer. Let E_i be a subset of memory tuples in E at which arm i was played, and let n_i be its size. We denote by $E_{\phi^{old}}^i \in \mathbb{R}^{n_i \times g}$ a matrix whose rows are feature vectors that were played by arm i . After a training phase is completed, we evaluate the new activations on the same replay buffer and denote the equivalent set by $E_\phi^i \in \mathbb{R}^{n_i \times g}$.

Our approach is to summarize the knowledge that the algorithm has gained from exploring with the features ϕ^{old} into priors on the new features Φ_i^0, μ_i^0 . Once these priors are computed, we restart the linear TS algorithm using the data that is currently available in the replay buffer. For each arm i , let $\phi_j^i = (E_\phi^i)_j$ be the j -th row in E_ϕ^i and let r_j be the corresponding reward, we set $\Phi_i = \sum_{j=1}^{n_i} \phi_j^i (\phi_j^i)^\top$, $\psi_i = \sum_{j=1}^{n_i} \phi_j^i r_j$. We now explain how we compute Φ_i^0, μ_i^0 .

Recall that under Assumption 2, the likelihood of the reward

is approximately invariant to the choice of representation:

$$\mathbb{E}[r_i(t)|\phi(t)] \approx \phi(t)^\top \mu_i \approx \phi^{old}(t)^\top \mu_i^{old} \approx \mathbb{E}[r_i(t)|\phi^{old}(t)].$$

For all i , we define the estimator of the reward as $\theta_i(t) = \phi(t)^\top \tilde{\mu}_i(t)$. Due to the posterior distribution of $\tilde{\mu}_i(t)$, the marginal distribution of each $\theta_i(t)$ is $\mathcal{N}(\phi_i(t)^\top \hat{\mu}_i(t), \nu_i^2 s_{t,i}^2)$, where $s_{t,i} = \sqrt{\phi(t)^\top \Phi_i(t)^{-1} \phi(t)}$ (see Agrawal & Goyal (2013) for derivation). The goal is to match the likelihood of the reward estimation $\theta_i(t)$ given the new features to be the same as with the old features.

4.1 Approximation of the mean μ_i^0 : The DNN is trained to minimize the MSE (Eq 1). Given the new features ϕ , the current weights of the last layer of the DNN already make a good prior for μ_i^0 . In Levine et al. (2017), this approach was shown empirically to improve the performance of a neural-linear DQN. The main advantage is that the DNN is optimized online by observing the entire data and is therefore not limited to the current replay buffer. Thus, the weights of the current DNN hold information on more data and make a strong prior.

4.2 Approximation of the correlation matrix Φ_i^0 : For each arm i , our algorithm receives as input the sets of new and old features $E_\phi^i, E_{\phi^{old}}^i$ with elements $\{\phi_j^{old}, \phi_j\}_{j=1}^{n_i}$. In addition, the algorithm receives the correlation matrix Φ_i^{old} . Notice that due to our algorithm's nature, Φ_i^{old} holds information on contexts that are not available in the replay buffer. The goal is to find a correlation matrix, Φ_i^0 , for the new features that will have the same variance on past contexts as Φ_i^{old} . I.e., we want to find Φ_i^0 such that

$$\begin{aligned}s_{j,i}^2 &= \phi_j^\top (\Phi_i^0)^{-1} \phi_j = \text{Trace}((\Phi_i^0)^{-1} \phi_j \phi_j^\top) \\ &\quad \forall i \in [1..N], j \in [1..n_i],\end{aligned}$$

where $s_{j,i}^2 \doteq (\phi_j^{old})^\top (\Phi_i^{old})^{-1} \phi_j^{old}$ and the last equality follows from the cyclic property of the trace. For hand $i \in [1..N]$, we denote by $X_{j,i} \doteq \phi_j \phi_j^\top \in \mathbb{R}^{d \times d}$ the 1-rank symmetric matrix $\forall j \in [1..n_i]$. Using this definition, we have that

$$\text{Trace}((\Phi_i^0)^{-1} \phi_j \phi_j^\top) = \text{Trace}(X_{j,i}^\top (\Phi_i^0)^{-1})$$

is an inner product over the vector space of symmetric matrices, known as the Frobenius inner product. Finally, as $(\Phi_i^0)^{-1}$ is an inverse correlation matrix, we constrain the solution to be semi positive definite. Thus, the optimization problem is equivalent to a linear regression problem in the vector space of positive semi definite (PSD) matrices for all actions $i \in [1..N]$:

$$\begin{aligned}\underset{(\Phi_i^0)^{-1}}{\text{minimize}} \quad & \sum_{j=1}^{n_i} (\text{Trace}(X_{j,i}^\top (\Phi_i^0)^{-1}) - s_{j,i}^2)^2 \\ \text{subject to} \quad & (\Phi_i^0)^{-1} \succeq 0.\end{aligned}\tag{2}$$

In practice, we solve the SDP by applying SGD using sampled batches from $E_{\phi^{old}}^i$ and E_{ϕ}^i . Each SGD iteration is followed by eigenvalues thresholding (denoted by $\text{EigenValueThresholding}((\Phi_i^0)^{-1})$) in order to project $(\Phi_i^0)^{-1}$ back to PSD matrices space. To avoid evaluating E_{ϕ}^i each time the DNN is updated, we take advantage of the iterative learning phase of the DNN and the iterative nature of the SGD by using the same batch to update the DNN weights and $(\Phi_i^0)^{-1}$ simultaneously. In each iteration, we treat the inverse correlation matrix from the previous iteration as $(\Phi_i^{old})^{-1}$ and also as the initial guess for the current gradient decent step. For each action $a \in A$, we use a subset of the batch, in which action a was used.

Computational complexity. We consider the algorithm’s time and memory complexity and their dependence on different parameters of the problem. Recall that the last layer’s dimension is $g < d$ where d is the dimension of the raw features, the size of the limited memory buffer is n , the batch size is B , and the number of contexts seen by the agent is T . For the approximate SDP, each gradient step is Bg^2 (matrix-vector multiplications) plus the thresholding operator, which has a time complexity of $O(g^3)$ due to the matrix eigendecomposition. This can be improved in the case of low-rank stochastic gradients ($B < g$) into $O(g^2)$ as suggested in [Chen et al. \(2014\)](#). In addition, we use the contexts at our memory buffer to compute Φ_i after the prior matching, which is $O(n)$. The overall complexity is $O(T(g^2 + n))$ with a memory complexity of $O(n)$.

On the other hand, the computational complexity of the full memory approach results is $O(T^2)$, and the memory complexity is $O(T)$. This is because it is estimating the TS posterior using the complete data every time the representation changes. Due to the stochastic behavior of our SGD modification, the computational complexity is linear in the batch size and not in $|A|$.

To summarize, our method is more efficient than the full memory baseline in problems with a lot of data ($T \gg g^2$ and $T \gg n$). Instead of solving an SDP after each update phase (which is computationally prohibitive in general), we apply an efficient SGD in parallel to the DNN updates. This is also sample efficient due to the reuse of the same batch for both tasks. In our experiments, we noticed that using only 1 update iteration ($P = 1$) for both the DNN and likelihood matching is enough to get competitive results. Therefore, this is our default configuration.

4. Experiments

In this section, we empirically investigate the performance of the proposed algorithm to address the following questions:

- Does the NTK assumption holds? (i.e., does representa-

tion drift occurs?)

- Is our method sensitive to the memory buffer size?
- Can neural-linear bandits explore efficiently while learning representations under finite memory constraints?
- Does the moment matching mechanism allow neural-linear bandits to avoid catastrophic forgetting?
- Can the method be applied in a wide range of problems and across different DNN architectures?

We address these questions by performing experiments on ten real-world datasets, including high dimensional natural language data on a task of sentiment analysis from text, in which we evaluate our algorithm on a text-based dataset using CNNs. All of these datasets are publicly available through the Machine Learning Repository ¹.

Methods and setup. We experimented with different ablations of our approach, as well as a few baselines:

(1) **Linear TS** ([Agrawal & Goyal, 2013](#), Alg 1) using the raw context as a feature, with an additional uncertainty in the variance ([Riquelme et al., 2018](#)).

(2) **Neural-Linear TS** ([Riquelme et al., 2018](#)) the full memory version, in which the moments are computed each time the network is updated using all history.

(3) **NeuralUCB** ([Zhou et al., 2020](#)) an NTK approach that uses UCB based exploration for a general reward function. This method chooses the action that maximizes the upper confidence bound (similar to [Li et al. \(2010\)](#)) but uses the network gradients as features and the network output as the mean reward estimator. The NTK assumptions claim that the network parameters stay very close to the initialization point under some conditions (most notably- the network width). Thus, it enables them to estimate the covariance matrix by accumulating the features’ outer-product without recalculating them again.

(4) **NeuralTS** ([Zhang et al., 2020](#)) an NTK approach that uses TS based exploration for a general reward function. Like NeuralUCB, they use the estimated covariance matrix and the estimated mean to sample the reward for each arm and take the arm with the highest score. For more information regarding NeuralUCB and NeuralTS and their regret analysis, we refer the readers to [Zhang et al. \(2020\)](#) and [Zhou et al. \(2020\)](#). Both NeuralUCB and NeuralTS implementations are based on the official code provided by the authors ².

(5) Our limited memory neural-linear TS algorithm with likelihood matching (**NeuralLinearTS-LM**).

¹<https://archive.ics.uci.edu/ml/index.php>

²<https://github.com/ZeroWeight/NeuralTS>



Figure 1. An illustration of catastrophic forgetting due to limited memory without likelihood matching. The graph present mistake percentage at each round.

(6) An ablative version of (5) that calculates the prior only for the mean, similar to [Levine et al. \(2017\)](#).

(7) An ablative version of (5) that does not use prior calculations.

(8) Limited memory neural-linear TS with NTK assumption. This is the NTK version of our algorithm in which we do not perform likelihood matching (**NeuralLinearTS-NTK**) but still accumulate features without resetting the priors.

Algorithms 5-8 make an ablative analysis for the limited memory neural-linear approach. As we will see, adding each one of the priors improves learning and exploration. As noted, in all versions of our algorithm, we update the network each round with one iteration, while in the full-memory version, we train the network every 400 rounds with 800 iterations due to the large computational burden that makes every round update prohibited. The full-memory NTK based algorithms (3-4) are trained every round with at most 1000 iterations as their official code dictates. Note that in both cases, the overall number of training iterations is larger than our algorithm. In all the experiments, we used the same hyperparameters as in [Riquelme et al. \(2018\)](#). E.g., the network architecture is an MLP with a single hidden layer of size 50. The only exception is the text CNN (details below). The size of the **memory buffer** is set to be 100 per action for the limited memory algorithms, and the batch size is set to be 16 times the number of actions. The initial learning rate for both the DNN training and the moments matching was set to 0.01 with a decaying factor of $1/t$.

4.1. Representation drift

First, we examine the amount of change in the representation ϕ during the training of f_ω . To do so, we compute the NTK, denoted by K , for two fixed contexts b and b' during training with the Shuttle Statlog dataset ([Newman et al., 2008](#)) for various network widths: 50, 100, 500, 1024. The results and the experiment for $K(b', b')$ are presented in Fig 2. More results are presented in the Supplementary Material. As can be noted, for wider networks, the NTK

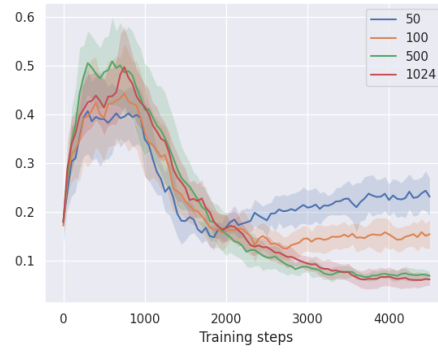


Figure 2. Graph of the NTK during training for various network widths.

converges during the training session. Nevertheless, for a significant part of the training, the kernel changes, and the NTK assumption does not hold, which may cause a non-optimal performance. Therefore, a representation drift occurs, and our likelihood matching mechanism is justified. This is of particular importance when exploration and representation learning are done simultaneously as opposed to standard learning problems where no exploration is needed.

4.2. Catastrophic forgetting

Next, we examine the impact of catastrophic forgetting on the algorithm’s performance on the Statlog dataset. We add a version of the limited memory without moments matching in which the training is done in phases of 400 steps, similar to the limited-memory variation in [Riquelme et al. \(2018\)](#). We ran the experiment with a memory size of 100 for all limited memory versions to emphasize performance degradation.

Fig 1 shows the performance of each of the algorithms in this setup. We let each algorithm run for 4000 steps (contexts) and average each algorithm over 10 runs. The x-axis corresponds to the number of contexts seen so far, while

Name	d	A	Full memory		Limited memory			NTK based		
			LinearTS	NeuralLinearTS	NeuralLinearTS-LM	Only mean	No prior	NeuralUCB	NeuralTS	NeuralLinearTS-NTK
Mushroom	117	2	1.000	0.985	0.945	0.719	0.730	0.521	0.521	0.941
Financial	21	8	0.997	0.946	1.000	0.743	0.723	0.292	0.228	0.959
Jester	32	8	1.000	0.784	0.819	0.287	0.234	0.546	0.546	0.768
Adult	88	2	0.977	0.974	1.000	0.638	0.634	0.822	0.823	0.966
Covertime	54	7	1.000	0.902	0.892	0.679	0.693	0.514	0.517	0.887
Census	377	9	0.548	0.860	1.000	0.679	0.686	0.644	0.603	0.863
Statlog	9	7	0.912	0.978	1.000	0.933	0.916	0.818	0.885	0.976
Epileptic	178	5	0.282	1.000	0.684	0.562	0.504	0.019	0.020	0.589
Smartphones	561	6	0.649	0.970	1.000	0.521	0.515	0.396	0.670	0.965
Scania Trucks	170	2	0.181	0.672	0.745	-0.344	-0.050	0.988	1.000	0.259
Amazon	7K	5	-	0.986	1.000	0.873	0.879	-	-	0.981
Average			0.755	0.914	0.917	0.572	0.588	0.556	0.581	0.832
Median			0.945	0.970	1.000	0.679	0.686	0.534	0.575	0.941

Table 1. Normalized cumulative reward of algorithms on 11 real world datasets. The context dim d and the size of the action space A are reported for each dataset. The result of each algorithm is reported for 10 runs.

the y-axis measures the instantaneous regret (lower is better). The cumulative reward achieved by each algorithm averaged over seeds can be found in Table 1 (Statlog); in Fig 1 we focus on the qualitative behavior, as described below. First, we can see that the neural-linear method (blue) outperforms the linear one (brown), suggesting that this dataset requires a nonlinear function approximation. We can also see that our likelihood matching method allows the limited memory algorithm (orange) to perform almost as well as the neural-linear algorithm without memory constraints (blue) while our algorithm operates online.

In addition, the limited memory neural-linear algorithms that do not perform likelihood matching (purple and red) suffer from "catastrophic forgetting" due to limited memory. Intuitively, the covariance matrix holds information regarding the number of contexts seen by the agent and used by the algorithm for exploration. When no such prior is available, the agent explores sub-optimal arms from scratch every time the features are modified. In the online version (red), the representation is changed each round, which makes the agent act consistently sub-optimally. Alternatively, in the phase-based version (purple), we see a degradation each time the agent trains (every 400 steps, marked by the x-ticks on the graph). Indeed, we observe "peaks" in the regret curve for this algorithm. This is significantly reduced when we compute the prior on the covariance matrix (orange), making the limited memory neural-linear bandit resilient to catastrophic forgetting. The NTK based version (green) acts well but suffers from a "slow" starting due to the representation drift. In the next experiments, we will see that our algorithm performs better overall.

4.3. Memory size ablation study

We evaluate the impact of the memory size on our algorithm. We ran our algorithm with various memory sizes against a limited memory neural-linear without moment matching

and checked their performance on the Statlog dataset. For every memory size, we ran the algorithms for 10 times. The results are depicted in Fig 3. As can be noted, the algorithm performance is not sensitive to the memory size, and its performance across different memory sizes stays high. On the other hand, a version without likelihood matching is deeply sensitive to the memory size due to catastrophic forgetting. Note that the variance margin of the method without likelihood matching is so small compared to the magnitude of the mean, that is not visible in the figure.

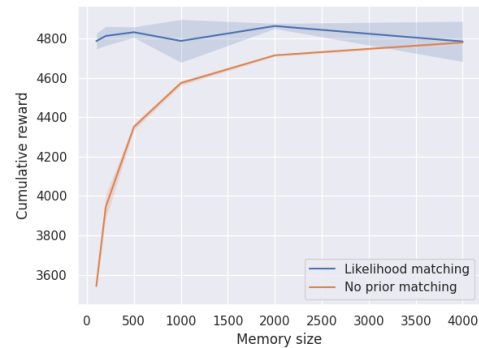


Figure 3. Cumulative reward on the Statlog dataset for various memory sizes.

4.4. Real world data

We evaluate our approach on ten real-world datasets and another high-dimensional text dataset (details at the next subsection); for each dataset, we present the cumulative reward achieved by each algorithm, averaged over 10 runs. Each run was performed for 5000 steps. Due to the fact that each dataset behaves differently in terms of difficulty and maximum possible cumulative reward, we normalize the scores

for each dataset according to: $normalized\ score(i) = \frac{score(i) - R}{\max_i score(i) - R}$, where R is the mean cumulative reward of a random policy. We also present the average and median values for each algorithm. The raw results are presented in the Supplementary Material.

Inspecting Table 1, we can see that using our limited memory algorithm with likelihood matching (NeuralLinearTS-LM), improved the performance of the limited memory neural-linear variations, in which we do not update the priors (Only mean/ No prior). Furthermore, in some cases, NeuralLinearTS-LM even outperformed the full memory neural-linear algorithm by a small margin. This can be explained by the fact that limited memory with prior matching behaves as an implicit regularizer by adding noise to the learning. Scania Trucks’s results are particularly interesting because the ablative versions (without prior updating) act worse than a random policy, which performs surprisingly well (4663 out of 5000). These findings suggest that likelihood matching improves performance and makes the algorithm resilient to catastrophic forgetting.

In some of the datasets, we observed that a linear baseline (LinearTS) performed well. This suggests that there is no need for a deep representation of the contexts, and that a linear function is good enough to model each hand’s reward. A linear algorithm can use finite memory in these cases and does not need to match the likelihood. However, as can be concluded from our results, the reward function is generally non-linear, in which case the linear baseline performs poorly. Nevertheless, even in some datasets where LinearTS performs well, NeuralLinearTS-LM outperforms it.

The last part of the table shows the results for the NTK based methods. Clearly, NeuralUCB and NeuralTS are outperformed by our algorithm for most datasets (except Scania Trucks) and poorly perform on the linear datasets. Moreover, NeuralLinearTS-NTK shows great performance and outperforms NeuralUCB and NeuralTS, which can be explained by the fact that NeuralUCB and NeuralTS perform the exploration on the entire network parameter space instead of the last layer as done in the neural-linear case. This makes the problem more complex and harder to solve.

Nevertheless, our algorithm NeuralLinearTS-LM also outperforms NeuralLinearTS-NTK on all datasets. Note that at the Census dataset, a complex dataset in terms of action number and dimensions, the performance gap between the NTK version and our algorithm is significant because the representation problem is harder, and there is a bigger change in the representation during training. These results indicate that our method successfully copes with representation drift.

4.5. Sentiment analysis from text using CNNs

This is an experiment on the ”Amazon Reviews: Unlocked Mobile Phones” dataset. This dataset contains reviews of unlocked mobile phones sold on ”Amazon.com”. The goal is to determine the rating (1 to 5 stars) of each review using only the text itself. We use our model with a Convolutional Neural Network (CNN) suited to NLP tasks (Kim, 2014; Zakhavy et al., 2018b). Specifically, the architecture is a shallow word-level CNN that was demonstrated to provide state-of-the-art results on various classification tasks by using word embeddings while not being sensitive to hyperparameters (Zhang & Wallace, 2015). We use the architecture with its default hyper-parameters and standard pre-processing (e.g., we use random embeddings of size 128, and we trim and pad each sentence to a length of 60). The only modification we made was to add a linear layer of size 50 to make the size of the last hidden layer consistent with previous experiments. The results are in Table 1 marked in yellow.

In this experiment, the input dimension is large (\mathbb{R}^{7K}), so we could not run the linear baseline since it is not computationally practical in these dimensions. We compare the proposed method – neural-linear with finite memory and likelihood matching with the full memory neural-linear TS baseline, limited memory without moment matching baselines, and neural-linear NTK based baseline (although the NTK assumptions do not apply for CNNs). Looking at Table 1, we can see that the limited memory version without likelihood matching performs as good as the full memory and better than the other baselines.

5. Summary

We presented a complementary method for neural-linear contextual bandit with limited memory that succeeds to solve representation drift during exploration, a problem that occurs at NTK based algorithms. Our method is able to do so while being resilient to catastrophic forgetting, which is a major drawback of former limited memory approaches. Moreover, we show an efficient way to implement our method by approximately solving an SDP using SGD so that only a single gradient step for both the learning and likelihood matching at each round is sufficient. Thus, our method is both memory and computationally efficient, which enables it to operate online. Our method demonstrated excellent performance on multiple real-world datasets, while its performance did not deteriorate due to the representation changes and limited memory.

We believe that our findings constitute an important step towards solving contextual bandit problems where both exploration and representation learning play essential roles. The main avenue for future work is to extend the ideas presented in this paper to Bayesian RL, where the imme-

diate reward is replaced by the return, perhaps focusing on Markov decision processes with fast mixing time (e.g. (Zintgraf et al., 2019)) or situations in which decisions are infrequent (e.g. decision after a stream of observations) where recurrent models can be used.

An interesting future work would be to examine the effect of the network architecture on the performance of contextual bandits DNN-based algorithms such as ours and perhaps consider ways to choose the DNN architecture for contextual bandits problems as opposed to this work where the network’s architecture is built for supervised learning, which in general may not be optimal for bandit problems.

References

- Abbasi-Yadkori, Y., Pal, D., and Szepesvari, C. Improved algorithms for linear stochastic bandits. In *Advances in Neural Information Processing Systems*, pp. 2312–2320, 2011.
- Agrawal, S. and Goyal, N. Thompson sampling for contextual bandits with linear payoffs. In *International Conference on Machine Learning*, pp. 127–135, 2013.
- Auer, P. Using confidence bounds for exploitation-exploration trade-offs. *Journal of Machine Learning Research*, 3(Nov):397–422, 2002.
- Azizzadenesheli, K., Brunskill, E., and Anandkumar, A. Efficient exploration through bayesian deep q-networks. *arXiv preprint arXiv:1802.04412*, 2018.
- Bellemare, M., Srinivasan, S., Ostrovski, G., Schaul, T., Saxton, D., and Munos, R. Unifying count-based exploration and intrinsic motivation. In *Advances in Neural Information Processing Systems*, pp. 1471–1479, 2016.
- Chen, J., Yang, T., and Zhu, S. Efficient low-rank stochastic gradient descent methods for solving semidefinite programs. In *Artificial Intelligence and Statistics*, pp. 122–130, 2014.
- Chu, W., Li, L., Reyzin, L., and Schapire, R. Contextual bandits with linear payoff functions. In *Proceedings of the Fourteenth International Conference on Artificial Intelligence and Statistics*, pp. 208–214, 2011.
- Goodfellow, I., Bengio, Y., and Courville, A. *Deep learning*. MIT press, 2016.
- Jacot, A., Gabriel, F., and Hongler, C. Neural tangent kernel: Convergence and generalization in neural networks. In *Advances in neural information processing systems*, pp. 8571–8580, 2018.
- Kim, Y. Convolutional neural networks for sentence classification. *arXiv preprint*, 2014.
- Kirkpatrick, J., Pascanu, R., Rabinowitz, N., Veness, J., Desjardins, G., Rusu, A. A., Milan, K., Quan, J., Ramalho, T., Grabska-Barwinska, A., Hassabis, D., Clopath, C., Kumaran, D., and Hadsell, R. Overcoming catastrophic forgetting in neural networks. *Proceedings of the National Academy of Sciences*, 114(13): 3521–3526, 2017. ISSN 0027-8424. doi: 10.1073/pnas.1611835114. URL <https://www.pnas.org/content/114/13/3521>.
- Langford, J. and Zhang, T. The epoch-greedy algorithm for multi-armed bandits with side information. In *Advances in neural information processing systems*, pp. 817–824, 2008.
- Lattimore, T. and Szepesvári, C. *Bandit algorithms*. 2018.
- LeCun, Y., Bengio, Y., and Hinton, G. Deep learning. *nature*, 521(7553):436, 2015.
- Levine, N., Zahavy, T., Mankowitz, D. J., Tamar, A., and Mannor, S. Shallow updates for deep reinforcement learning. In *Advances in Neural Information Processing Systems*, pp. 3135–3145, 2017.
- Li, L., Chu, W., Langford, J., and Schapire, R. E. A contextual-bandit approach to personalized news article recommendation. In *Proceedings of the 19th international conference on World wide web*, pp. 661–670. ACM, 2010.
- Mnih, V., Kavukcuoglu, K., Silver, D., Rusu, A. A., Veness, J., Bellemare, M. G., Graves, A., Riedmiller, M., Fidjeland, A. K., Ostrovski, G., et al. Human-level control through deep reinforcement learning. *Nature*, 518(7540): 529–533, 2015.
- Newman, D., Smyth, P., Welling, M., and Asuncion, A. U. Distributed inference for latent dirichlet allocation. In *Advances in neural information processing systems*, pp. 1081–1088, 2008.
- O’Donoghue, B., Osband, I., Munos, R., and Mnih, V. The uncertainty bellman equation and exploration. *International Conference on Machine Learning*, 2018.
- Osband, I., Aslanides, J., and Albin, C. Randomized prior functions for deep reinforcement learning. *Advances in Neural Information Processing Systems*, 2018.
- Pathak, D., Agrawal, P., Efros, A. A., and Darrell, T. Curiosity-driven exploration by self-supervised prediction. In *International Conference on Machine Learning*, 2017.
- Riquelme, C., Tucker, G., and Snoek, J. Deep bayesian bandits showdown. In *International Conference on Learning Representations*, 2018.
- Russo, D. J., Van Roy, B., Kazerouni, A., Osband, I., Wen, Z., et al. A tutorial on thompson sampling. *Foundations and Trends® in Machine Learning*, 11(1):1–96, 2018.
- Silver, D., Huang, A., Maddison, C. J., Guez, A., Sifre, L., van den Driessche, G., Schrittwieser, J., Antonoglou, I., Panneershelvam, V., Lanctot, M., Dieleman, S., Grewe, D., Nham, J., Kalchbrenner, N., Sutskever, I., Lillicrap, T., Leach, M., Kavukcuoglu, K., Graepel, T., and Hassabis, D. Mastering the game of Go with deep neural networks and tree search. *Nature*, 529(7587):484–489, jan 2016. ISSN 0028-0836. doi: 10.1038/nature16961.

- Thompson, W. R. On the likelihood that one unknown probability exceeds another in view of the evidence of two samples. *Biometrika*, 25(3/4):285–294, 1933.
- Vandenberghe, L. and Boyd, S. Semidefinite programming. *SIAM review*, 38(1):49–95, 1996.
- Xu, P., Wen, Z., Zhao, H., and Gu, Q. Neural contextual bandits with deep representation and shallow exploration. *arXiv preprint arXiv:2012.01780*, 2020.
- Zahavy, T., Haroush, M., Merlis, N., Mankowitz, D. J., and Mannor, S. Learn what not to learn: Action elimination with deep reinforcement learning. *Advances in Neural Information Processing Systems*, 2018a.
- Zahavy, T., Magnani, A., Krishnan, A., and Mannor, S. Is a picture worth a thousand words? a deep multi-modal fusion architecture for product classification in e-commerce. *The Thirtieth Conference on Innovative Applications of Artificial Intelligence (IAAI)*, 2018b.
- Zhang, W., Zhou, D., Li, L., and Gu, Q. Neural thompson sampling. *arXiv preprint arXiv:2010.00827*, 2020.
- Zhang, Y. and Wallace, B. A sensitivity analysis of (and practitioners’ guide to) convolutional neural networks for sentence classification. *arXiv preprint arXiv:1510.03820*, 2015.
- Zhou, D., Li, L., and Gu, Q. Neural contextual bandits with ucb-based exploration. In *International Conference on Machine Learning*, pp. 11492–11502. PMLR, 2020.
- Zintgraf, L., Shiarlis, K., Igl, M., Schulze, S., Gal, Y., Hofmann, K., and Whiteson, S. Varibad: A very good method for bayes-adaptive deep rl via meta-learning. *arXiv preprint arXiv:1910.08348*, 2019.

Online Limited Memory Neural-Linear Bandits with Likelihood Matching - Supplementary Material

A. Pseudo code

Algorithm 2 Limited Memory Neural-linear TS with Likelihood Matching

Set $\forall i \in [1, \dots, N] : \Phi_i^0 = I_d, \hat{\mu}_i = \mu_i^0 = 0_d, \Phi_i = 0_{d \times d}, \psi_i = 0_d$
Initialize Replay Buffer E , and DNN f
Define $\phi(t) \leftarrow \text{LastLayerActivations}(f(b(t)))$
for $t = 1, 2, \dots$, **do**
 Observe $b(t)$, evaluate $\phi(t)$
 Posterior sampling: $\forall i \in [1, \dots, N]$, sample $\tilde{\mu}_i(t) \sim N(\hat{\mu}_i, \nu^2(\Phi_i^0 + \Phi_i)^{-1})$
 Play arm $a(t) := \text{argmax}_i \phi(t)^\top \tilde{\mu}_i(t)$, **Observe** reward r_t and **Store** $\{b(t), a(t), r_t\}$ in E
 if E is full **then**
 Remove the first tuple in E with $a = a(t)$ (round robin)
 end if
 for P steps **do**
 Sample batch $\{b_j, a_j, r_j\}_{j=1}^B$ from E
 Compute old features $\{\phi_j^{old}\}_{j=1}^B$
 Optimize ω on $\nabla_\omega \mathcal{L}_{NN}$ and compute new features $\{\phi_j\}_{j=1}^B$
 $(\Phi_i^0)^{-1} \leftarrow (\Phi_i^0 + \Phi_i)^{-1}$
 for $\forall i \in [1, \dots, N]$ **do**
 $e_i^{old} \leftarrow \{\phi_j^{old} | a_j = i\}, e_i \leftarrow \{\phi_j | a_j = i\}$
 $(\Phi_i^0)^{-1} \leftarrow \text{ProjectedGradientDecent}((\Phi_i^0)^{-1}, e_i^{old}, e_i, \alpha)$
 end for
 end for
 for $\forall i \in [1, \dots, N]$ **do**
 Use the current weights of the last layer of the DNN as a prior for μ_i^0
 $\Phi_i = \sum_{j=1}^{n_i} \phi_j^i (\phi_j^i)^\top, \psi_i = \sum_{j=1}^{n_i} (\phi_j^i)^\top r_j$.
 end for
 Posterior update:
 $\Phi_{a(t)} = \Phi_{a(t)} + \phi(t)\phi(t)^\top, \psi_{a(t)} = \psi_{a(t)} + \phi(t)r_t, \hat{\mu}_{a(t)} = (\Phi_{a(t)}^0 + \Phi_{a(t)})^{-1} \left(\Phi_{a(t)}^0 \mu_{a(t)}^0 + \psi_{a(t)} \right)$
end for

Algorithm 3 ProjectedGradientDecent

Inputs: A_0 - PSD matrix, $\mathcal{B}_{old}, \mathcal{B}, \alpha$
Set $A \leftarrow A_0$
for $\phi_j^{old} \in \mathcal{B}_{old}$ and $\phi_j \in \mathcal{B}$ **do**
 Gradient step:
 $s_j^2 \leftarrow (\phi_j^{old})^\top A_0 \phi_j^{old}, X_j \leftarrow \phi_j (\phi_j)^\top$
 $A \leftarrow A - \alpha \nabla_A (\text{Trace}(X_j^\top A) - s_j^2)^2$
 Projection step:
 $A \leftarrow \text{EigenValueThresholding}(A)$
end for

B. Representation drift experiment

The NTK was sampled during training with the Shuttle Statlog dataset (Newman et al., 2008). We compute the NTK for two fixed contexts b and b' , taken from the dataset. Each context is composed of 9 features describing the space shuttle flight. The goal is to predict the state of the radiator of the shuttle (the reward). There are $N = 7$ possible actions; for correct predictions the reward is $r = 1$ and $r = 0$ otherwise.

The weights of the network were initialized according to (Jacot et al., 2018). We ran the experiments for various network widths: 50, 100, 500, and 1024. The network was trained as described in the main paper (Method and setup) with a random policy. The NTK was sampled every 50 iterations during training. For the estimated reward of the first action. The graphs below present $K(b, b)$, $K(b', b')$ and $K(b, b')$ from left to right accordingly during training.



C. Raw results

Name	d	A	Full memory		Limited memory			NTK based		
			LinearTS	NeuralLinearTS	NeuralLinearTS-LM	Only mean	No prior	NeuralUCB	NeuralTS	NeuralLinearTS-NTK
Mushroom	117	2	11162 ± 1167	10810 ± 428	9880 ± 1776	4602 ± 1408	4843 ± 1228	-32 ± 3	-34 ± 18	9785 ± 1012
Financial	21	8	3752 ± 8	3560 ± 12	3762 ± 18	2802 ± 21	2726 ± 23	1116 ± 824	876 ± 595	3610 ± 18
Jester	32	8	15944 ± 170	14731 ± 304	14926 ± 571	11940 ± 1307	11647 ± 1066	13397 ± 7	13397 ± 8	14642 ± 200
Adult	88	2	4008 ± 14	4003 ± 12	4043 ± 15	3483 ± 33	3477 ± 16.5	3768 ± 2	3769 ± 2	3990 ± 17
Coverttype	54	7	2961 ± 25	2742 ± 40	2719 ± 62	2241 ± 30	2272 ± 37	1870 ± 11	1877 ± 83	2708 ± 31
Census	377	9	1801 ± 15	2510 ± 21	2827 ± 22	2099 ± 39	2114 ± 34	2019 ± 94	1926 ± 76	2517 ± 42
Statlog	9	7	4460 ± 19	4729 ± 6	4820 ± 68	4545 ± 34	4476 ± 19	4075 ± 3	4348 ± 265	4722 ± 12
Epileptic	178	5	1204 ± 29	1734 ± 46	1501 ± 115	1411 ± 30	1368 ± 26	1010 ± 2	1011 ± 2	1431 ± 47
Smartphones	561	6	3092 ± 18	4208 ± 23	4313 ± 46	2647 ± 17	2626 ± 16	2214 ± 1548	3166 ± 1113	4191 ± 32
Scania Trucks	170	2	4710 ± 171	4837 ± 132	4856 ± 111	4574 ± 220	4650 ± 103	4919 ± 19	4922 ± 23	4730 ± 179
Amazon	7K	5	-	3024 ± 25	3052 ± 160	2793 ± 41	2804 ± 41	-	-	3014 ± 37

Table 2. Cumulative reward on 11 real world datasets.